Pacemaker Control of Heart Rate Variability: A Cyber Physical System Perspective

PAUL BOGDAN, Carnegie Mellon University
SIDDHARTH JAIN, Indian Institute of Technology Kanpur
RADU MARCULESCU, Carnegie Mellon University

Cardiac diseases, like those related to abnormal heart rate activity, have an enormous economic and psychological impact worldwide. The approaches used to control the behavior of modern pacemakers ignore the fractal nature of heart rate activity. The purpose of this article is to present a Cyber Physical System approach to pacemaker design that exploits precisely the fractal properties of heart rate activity in order to design the pacemaker controller. Towards this end, we solve a finite horizon optimal control problem based on the heartbeat time series and show that this control problem can be converted into a system of linear equations. We also compare and contrast the performance of the fractal optimal control problem under six different cost functions. Finally, to get an idea of hardware complexity, we implement the fractal optimal controller on a Virtex4 FPGA and report some preliminary results in terms of area overhead.

Categories and Subject Descriptors: C.3 [**Computer Systems Organization**]: Special Purpose and Application-based Systems—*Process control systems, Real-time and embedded systems*; G.1.2 [**Mathematics of Computing**]: Numerical Analysis—*Wavelets and fractals*; I.2.8 [**Artificial Intelligence**]: Problem Solving, Control Methods, and Search; J.3 [**Computer Applications**]: Life and Medical Sciences—*Health*

General Terms: Algorithms, Human Factors, Theory, Design, Performance

Additional Key Words and Phrases: Cyber physical systems, heart rate variability, fractional calculus, optimal control, fractal behavior, non-stationary behavior

ACM Reference Format:
Bogdan, P., Jain, S., and Marculescu, R. 2013. Pacemaker control of heart rate variablility: A cyber physical system perspective. ACM Trans. Embedd. Comput. Syst. 12, 1s, Article 50 (March 2013), 22 pages.
DOI: http://dx.doi.org/10.1145/2435227.2435246

1. INTRODUCTION

Cyber Physical Systems (CPS) consist of a network of embedded computation and communication devices together with sensors that can monitor and control various physical processes [Lee 2010; Stankovic et al. 2005] (see Figure 1). Such physical processes can take place in medical devices (e.g., health care system for monitoring and diagnosis, drug delivery systems, robotic surgery), transportation systems (e.g., traffic control, collision avoidance), electric power and environmental control, energy generation and transportation, zero-net energy buildings, access to dangerous or inaccessible

---

P. Bogdan is currently affiliated with the University of Southern California.
This work is supported in part by the National Science Foundation under grant CCF-0916752.
Author's addresses: P. Bogdan, Ming Hsieh Department of Electrical Engineering, University of Southern California; S. Jain, Electrical Engineering Department, Indian Institute of Technology Kanpur; R. Marculescu, Electrical and Computer Engineering Department, Carnegie Mellon University; email: radum@ece.cmu.edu.

DOI: http://dx.doi.org/10.1145/2435227.2435246

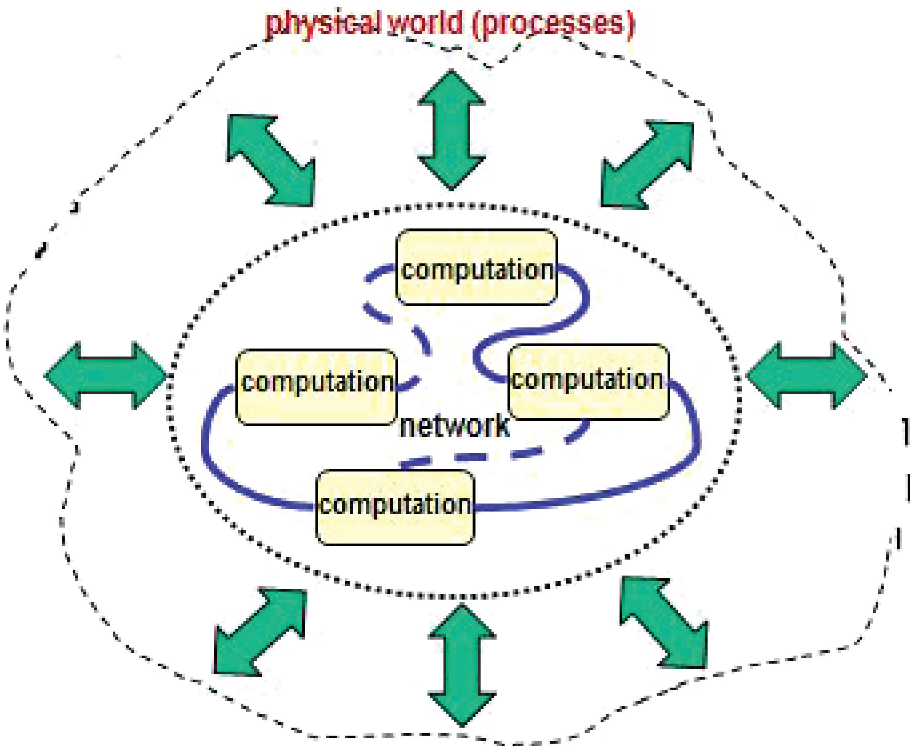

Fig. 1. CPS paradigm showing a network of computation devices interacting with physical world processes. The role of the computational components (e.g., sensors, audio/video cameras) of the CPS network is to collect and process information about various physical processes, communicate it via either wired (uninterrupted lines) or wireless (dotted lines) links to the decision centers, which in turn use this information for controlling the dynamics of physical processes or CPS components. The characteristics of physical processes are crucial for designing, optimizing and determining the CPS structure (e.g., required number of computational nodes to achieve a certain monitoring confidence) and its dynamics (e.g., finding the best communication scheduling with minimum energy overhead) [Bogdan and Marculescu 2011].

environments (e.g., autonomous systems for search and rescue, fire fighting and exploration), communication and financial networks, etc. [Sticherling et al. 2009].

In order to build CPS it is essential to know the system dynamics so time becomes an intrinsic component of the programming model of such systems. Also, CPS need to be low power, reliable, safe, real time, efficient and secure. Consequently, the theory of CPS design requires accurate modeling of physical processes so that they can be efficiently characterized and controlled over a heterogeneous network of sensor and computation devices [Bogdan and Marculescu 2011] (see Figure 1).

The CPS targeting health care applications need to be adaptive, autonomous, efficient, functional, reliable and safe. At the same time, they also need to maximize patient's quality-of-life, while minimizing the intrinsic costs of hospitalization. For instance, statistics from the Centre of Disease Control and Prevention predict more than 600,000 deaths per year due to cardiac issues. Therefore, it becomes necessary to build bio-implantable devices that are robust in monitoring and transmitting the heart rate to various medical devices or experts, as well as controlling the misbehavior of heart in real time [Jaegar 2010].

The development of CPS for health care applications has been significantly slowed down due to the lack of a coherent theory that can allow designers to comprehend and

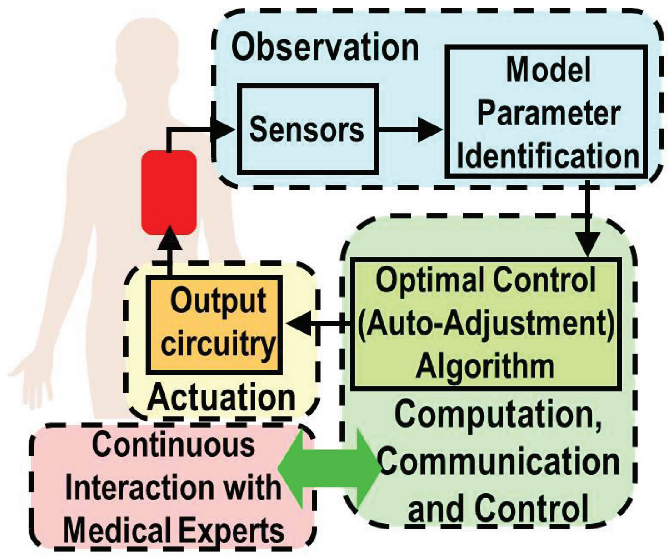

Fig. 2. CPS approach to pacemaker design. Interaction with medical experts/devices on a continuous basis helps better monitoring and control of the heart rate activity. The model identified is controlled through a suitable optimal control algorithm and the controlled output is fed back for heart pacing [Bogdan et al. 2012].

coordinate the cyber and physical resources in a unique, efficient, and robust approach. Such a CPS example is the artificial pacemaker, which is a medical device meant to regulate the heart rate using electrical impulses. In short, a pacemaker consists of both analog (i.e., sense amplifiers to monitor information about heart rate activity and pacing output circuitry) and digital components (i.e., microprocessors and memory blocks to actuate pacing events) [Haddad et al. 2006; Sanders and Lee 1996]. The control problem of an artificial pacemaker consists of first identifying the parameters of the heart model and then controlling its rate using a characteristic variable (e.g., content of venous oxygen, R-R time intervals, etc.) [Inbar et al. 1988; Hexamer et al. 2001; Zhang et al. 2002].

In Figure 2, we illustrate the idea of using a CPS approach to pacemaker design. As it can be seen, this consists of four important blocks, namely, the *Observation, Computation, Communication and Control, and Actuation*. The sensors in the *Observation* block gather the heart rate time series of the patient; this time series is later used to model the heart rate variability. Based on the parameters identified by modelling the heart rate variability, the role of the pacemaker control algorithm is to verify whether the heart rate is normal or inductive to a life threatening condition; if the later is true, then the control algorithm is supposed to bring it down to normal levels. The control algorithm computes the pacing frequency required to control the heart rate to a normal level of say 75 beats/min; by changing the parameters in the *cost function* used by the control algorithm, the time required to bring the heart rate down to a normal level can be reduced. The pacing frequency computed by the algorithm is then fed to the patient's heart via the pacemaker *Actuation* block.

Recent research suggests that heart rate variability of healthy individuals is neither periodic, nor fully chaotic, but instead characterized by universal fractal laws [Ivanov et al. 2001, 1999, 1998; Kiyono et al. 2009]. However, the control algorithms in current pacemakers are based on linear system theory [Doyle-III et al. 2011; Lopez et al. 2010; Nakao et al. 2001; Neogi et al. 2010] or neural networks [Sun et al. 2008]. Other limitations of current pacemakers come from the fact that all proposed pacing algorithms rely on optimal closed loop pacing algorithms that depend on the characteristics of individual's heart on short and long time scales, as well as adequate medical therapy (see Figure 2) [Coenan et al. 2008; Dell'orto et al. 2004; Schaldach 1998; Simantirakis et al. 2009].

Starting with these overarching ideas, our contributions in this article are: First, we propose a more accurate modeling of the heart rate variability via fractional differential equations. Second, we formulate the rate adaptive pacing algorithm as a model predictive control problem seeking to solve iteratively a constrained finite horizon optimal control with fractal state equations. Third, we compare and contrast various control approaches for designing pacemakers and give a sense of the hardware implementation complexity of such a fractal controller. Taken together, these new contributions demonstrate the power of taking a CPS approach towards designing such bio-implantable devices where the effects due to interactions among the cyber and physical components are important and cannot be ignored.

The remainder of this article is structured as follows: Section 2 summarizes the complex mechanism behind human heart rate activity, the main approaches for building demand pacemakers and the motivation for a fractal optimal control approach. Section 3 reviews the concept of fractional calculus that is needed to model the physical processes in pacemakers. Section 4 proposes a constrained finite horizon optimal control approach to regulate the dynamics of a fractal process (i.e., R-R intervals) considering six performance cost functions. Section 5 presents the goodness-of-fit analysis for two modeling approaches (i.e., a non-fractal approach based on classical integer order calculus and a fractal one based on fractional order differential equations) and the performance analysis of the proposed control problems. Also, the hardware complexity of such a fractional controller is discussed using a real FPGA platform. Section 6 concludes the article by summarizing our main contributions and suggesting a few future directions of research for more accurate dynamic optimization algorithms of such medical systems.

2. MOTIVATION AND PRIOR WORK

2.1. Cardiac Signals and Role of Pacemakers

The human heart is divided into four chambers: two atria (top chambers holding the blood) and two ventricles (bottom thick- walled chambers meant to help pumping the blood into the circulatory system). The heart collects the oxygenated blood from the lungs in the left atrium and the deoxygenated blood from the body in the right atrium. At the time of collection of blood in the atria, the myocardium and other specialized fibers are resting. This is followed by a muscle contraction, which results in a heartbeat when the oxygenated blood from the left ventricle flows into the body and the deoxygenated blood from the right ventricle flows into the lungs for oxygenation. This cycle repeats for every heartbeat and this way the normal circulation of blood flow is maintained. This cycle is also called *cardiac cycle* and is controlled by some complex electrical signals needed to maintain the heart rate within certain limits [Fauci et al. 2008; Li et al. 2012]. Any disturbance in this cycle may result in heart diseases like tachycardia (fast pacing) and bradycardia (slow pacing).

A *QRS complex* is generated when ventricles depolarize and a P-Wave is generated when atria depolarize. A cardiac cycle is characterized by the duration between two consecutive occurrences of the QRS complex; this R-R time interval (see Figure 3) is used by physicians to characterize the heartbeat.[1] The relation between the heartbeat and the R-R interval motivates us to use the R-R interval dynamics to solve a fractal

[1]An R-R interval of 1 second means a heart rate of 60 beats per minute.

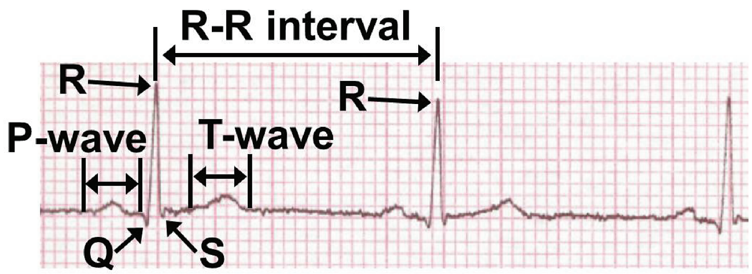

Fig. 3. A short electrocardiogram (ECG) showing the heart activity for three consecutive beats. The P-wave (atria depolarization), QRS complex (ventricular depolarization) and T-wave (ventricular repolarization) are shown. The R-R interval corresponds to the time elapsed between two consecutive heartbeats as a result of muscle contraction. The R-R interval dynamics is essential for medical diagnosis and pacemaker design and optimization.

optimal control problem that can control the heart rate in patients affected by some abnormalities.

2.2. Control Based Approaches to Pacemaker Design

Pacemakers were invented in 1932; since then, they have evolved from fixed rate pacemakers (i.e., pacemakers that deliver a pulse at fixed intervals of time) to demand pacemakers (i.e., pacemakers that deliver impulses only when a missing heartbeat is found). The control action in pacemakers plays a major part in demand pacemakers. For example, in the case of fast heart activity, if the pacemaker delivers an electrical impulse, this can become fatal to a patient as the heart cannot get enough time to supply the oxygenated blood and take the deoxygenated blood away from the body. In the case of lower heart rate, missing an electrical impulse can also turn out to be fatal since the body cannot get the oxygenated blood on time and then the cardiac cycle is disturbed.

Based on control approaches used and the state variables that are optimized, the *rate responsive* (or demand) pacemakers can be further divided into four main types namely: open loop (heart rate is defined based on current state using a predefined model without any feedback) [Alt et al. 1989; Bacharach et al. 1992; Humen et al. 1985; Stangl et al. 1989], closed loop (pacing rate is determined using a feedback loop that supplies information about the output) [Inbar et al. 1988; Jiang et al. 2011; Haddad et al. 2006; Hexamer et al. 2001; Hung 1990; Lee et al. 2011; Neogi et al. 2010; Sun et al. 2008; Zhang et al. 2002], metabolic (pacing depends on metabolism and or heart rate activity) [Lee et al. 2011; Nakao et al. 2001; Sugiura et al. 1983; Sugiura et al. 1991], and autonomous nervous system (ANS) controllers [Nakao et al. 2001]. For example, Inbar et al. [1988] describe a closed loop control approach where the content of venous oxygen is kept under a pre-defined saturation threshold needed to keep the heart rate under control. Along the same lines, [Hexamer et al. 2001] describe an approach in which atrio-ventricular conduction time (AVCT) is kept under control.

Zhang et al. [2002] also describe a closed loop approach that makes use of a proportional integrative derivative (PID) controller to reach a predefined R-R interval. A spiking neural network (SNN) based pacing device is proposed by Sun et al. [2008]; this device is also based on timing behavior of atrial and ventricular contraction, which is used to predict the pacing delays. In this model, a second order transfer function is used to determine the delays in the impulses delivered by SNN neurons. Neogi et al. [2010] model the heart rate activity by a second order transfer function and use a proportional plus derivative (PD) controller to control it. The basic assumption in all of these approaches is that they model the state variables via integer order differential equations.

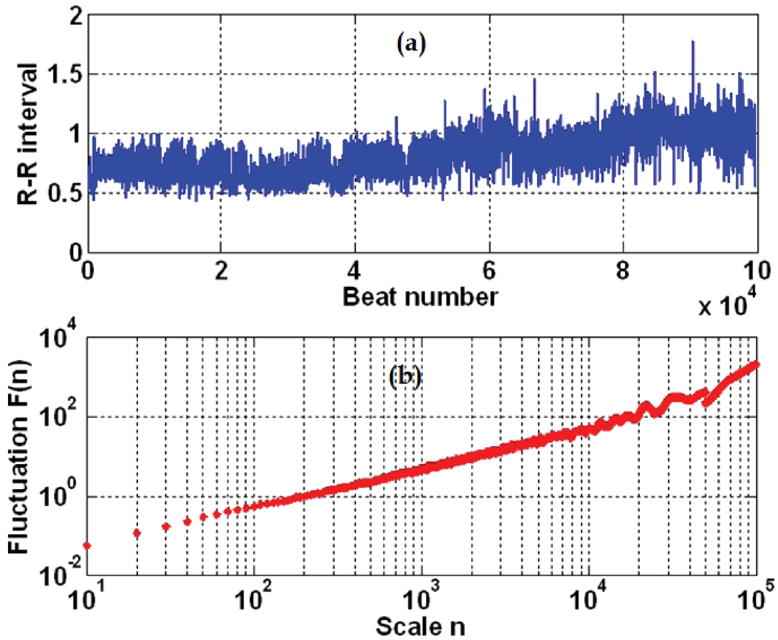

Fig. 4. (a) R-R interval variation as a function of heartbeat number. (b) Detrended fluctuation analysis $F(n)$ of R-R interval exhibits a linear behavior on log-log coordinates, which shows the fractal properties of the R-R interval.

Jiang et al. [2011] introduce a testing software platform that models the heart timing and electrical impulses via a finite state machine interfaced with a postulated pacemaker. The heartbeat control algorithm used by Lopez et al. in [Lopez et al. 2010] makes use of the concept of proportional gain and L_∞. [Sugiura et al. 1991] used fuzzy control theory for heart pacing using respiratory rate and temperature as state variables. On the other hand, Nakao et al. [2001] use blood pressure as state variable to regulate the heart rate.

Of note, all these approaches model heart rate or other physiological process via linear state equations. However, as can be seen in Figure 4(a), the process describing the heart rate activities is neither completely periodic, nor completely random. Indeed, by relying on detrended fluctuation analysis [Ivanov et al. 1998] and analyzing the fluctuations $F(n)$ as a function of scale n (see Figure 4(b)), one can observe the existence of linear scaling in log-log coordinates. This shows that the R-R intervals exhibit a fractal behavior that cannot be properly modeled using the integer order derivatives employed by classical control theory. Based on the above observations, we argue that the control algorithms for demand pacemakers should also rely on concepts rooted in fractional calculus and use a fractal model to describe the heart rate activity. Such an approach is described in the following sections.

3. BASICS OF FRACTIONAL CALCULUS

Fractional Calculus originates some hundreds of years back in some correspondence between L'Hospital and Leibniz where they argued over the meaning of introducing a 0.5 order differentiation [Podlubny 1999]. Since then, fractional calculus has found several applications in engineering (e.g., control [Oustaloup 1995; Podlubny 1999; Agrawal et al. 2010], bioengineering [Magin 2006]), physics (e.g., viscoelasticity

[Mainardi 2010], dielectric polarization [Onaral and Schwan 1982], and heat transfer [Battaglia et al. 2000]).

In short, *fractional (or fractal) calculus* incorporates integration and differentiation of arbitrary (i.e., non-integer) orders [Mandelbrot 2002; Podlubny 1999] of the dynamic characteristics of the target process $x(t)$ (e.g., R-R intervals, flow of oxygenated blood). This creates the difference between the integer order and the fractal calculus since, in the latter case, the process $x(t)$ can be represented as a *weighted sum* of the previous events $x(\tau)$, where $\tau \in (0, t]$:

$$ {}_{t_i}D_t^{\alpha} x(t) = \frac{d^{\alpha}x(t)}{dt^{\alpha}} = \frac{1}{\Gamma(n-\alpha)} \left(\frac{d}{dt}\right)^n \int_{t_i}^{t} (t-\tau)^{n-\alpha-1} x(\tau) d\tau. \tag{1} $$

In this representation, α is the fractional order of the derivative and $\Gamma(n-\alpha)$ is the Gamma function [Mandelbrot 2002]. This continuous definition has the following discrete time representation:

$$ {}_{t_i}D_t^{\alpha} x(t) = \frac{d^{\alpha}x(t)}{dt^{\alpha}} = \lim_{\Delta t \to 0} \frac{1}{\Delta t^{\alpha}} \sum_{j=0}^{[\frac{t-t_i}{\Delta t}]} w_{\alpha j} x(t - j\Delta t), \tag{2} $$

where $w_{\alpha j} = (-1)^j \binom{\alpha}{j}$, here $\binom{\alpha}{j} = \frac{\alpha(\alpha-1).....(\alpha-j+1)}{j(j-1).......1}$, Δt is the time increment, $[(t-t_i)/\Delta t]$ represents the integer part of $(t-t_i)/\Delta t$. From these equations, it can be clearly seen that the role of power law in time difference is directly captured in both Equation (1) and Equation (2); this way, a more accurate description of the heart rate variability process can be achieved and also better optimization becomes possible. We discuss these aspects in the next section.

4. FRACTIONAL CALCULUS BASED MODELING AND OPTIMAL CONTROL OF HEART ACTIVITY

In this section, we consider a constrained finite horizon optimal control problem. More precisely, given an initial time t_i and final time t_f, the optimal control tries to find the pacing frequency such that the cost function is minimized with a constraint on heart rate following the fractional dynamics. Note that the proposed formalism can be applied to other state and control variables as long as the state corresponds to a fractal physiological process (e.g., respiration, brain activity); it is evident here that modeling of heart rate via fractional differential equations corresponds to the *model parameter identification block* as shown in Figure 2.

Now we turn our attention to the cost functions. In the design of an optimal controller, there are two major quantities that determine the effectiveness of the designed controller, i.e., the error and the time at which the error compared to a reference value reaches the $y\%$ level [Schultz and Rideout 1961; Graham and Lathrop 1953]. The time at which the error reaches the $y\%$ level is defined as the minimum time after which the error is not more than $y/2\%$ compared to the reference value. In general the value of y is chosen to be 1, 2 or 5; we have chosen it to be 1% in our analysis. In our case, the error specifies the difference between the actual heart rate and the reference heart rate suggested by a physician as a result of some medical investigations. Consequently, this error is most of the time included in the cost function of the optimal controller. In [Schultz and Rideout 1961; Graham and Lathrop 1953] an entire class of cost functions that take the error and time as optimization penalties have been discussed. It is worth mentioning, that the finite horizon fractal optimal control that we discuss next corresponds to the *optimal control algorithm* block in Figure 2. In our case, we have considered the optimal control of heart rate under six different cost functions that can correspond to various medical conditions.

4.1. Finite Time Fractal Optimal Control with Integral of Squared Tracking Error Criterion (ISE)

The cost function which needs to be minimized in this case is as follows:

$$\min_{f(t)} \frac{1}{2} \int_{t_i}^{t_f} [w(t)(x(t) - x_{ref})^2 + z(t) f(t)^2] dt \tag{3}$$

subject to the following constraints:

$$_{t_i}D_t^{\alpha} x(t) = a(t)x(t) + b(t) f(t) \tag{4}$$

$$0 \leq x_{min} \leq x(t) \leq x_{max}, x(t_i) = x_0, x(t_f) = x_{ref} \tag{5}$$

$$f_{min} \leq f(t) \leq f_{max}, \tag{6}$$

where $x(t)$ represents the heart rate activity seen as a state variable, x_{ref} denotes the reference value that needs to be achieved in terms of heart rate activity, $f(t)$ is the pacing frequency, w and z are the weighting coefficients for the quadratic error and magnitude of the control signal, respectively.

In this formulation, α is the exponent of the fractional order derivative characterizing the dynamics of the heart rate activity $x(t)$, $a(t)$ and $b(t)$ are weighting coefficients for the heart activity and pacing frequency. Here α, $a(t)$ and $b(t)$ are dependent on the R-R interval dynamics, so these are physical variables (dependent on physical process), while the weighting coefficients w and z in Equation (3) can be manipulated by the CPS designer to ensure a fast convergence of R-R interval to the reference value. The effect of w on the convergence rate is discussed in the latter part of Section 5.2, and it is shown in Figures 11 and 12.

In addition, x_{min} and x_{max} are the minimum and maximum bounds on heart rate activity $x(t)$, $x(t_i)$ is the initial condition, $x(t_f)$ is the final condition, f_{min} and f_{max} are the minimum and maximum allowed bounds on pacing frequency $f(t)$.

By focusing on the squared of error in Equation (3), the optimal controller tries to find the pacing frequency such that both positive and negative deviations from the reference value for the R-R interval are minimized. The use of the integral of squared error between the actual and the reference heart rate is also attractive due to the following reasons: 1) It simplifies to linear equations when solving the optimal conditions. 2) The ISE criteria is in general robust to parameter variations. In this setup, we have to deal with very specific initial and final values summarized in Equation (5). Consequently, the role of the controller is to determine the right pacing frequency so as to bring the heart rate from a life threatening rate (x_0) to a final normal heart rate (x_{ref}), which can be suggested by medical experts.

To prevent the heart muscle be driven at an excessive pacing rate, we have to impose the conditions on the R-R interval and pacing frequency as given by Equations (4) and (6), respectively.

To solve this optimal control problem, we use the concept of Lagrange multipliers as follows:

$$\begin{aligned} L(x, f, w, z, \beta_1, \xi_1, \beta_2, \xi_2, \lambda) = & \int_{t_i}^{t_f} \left\{ \frac{w(t)(x(t) - x_{ref})^2}{2} + \frac{z(t) f(t)^2}{2} + \beta_1 (f - f_{min} - \xi_1) \right. \\ & \left. + \beta_2 (f_{max} - f - \xi_2) - \lambda \left[\frac{d^{\alpha} x(t)}{dt^{\alpha}} - a(t)x(t) - b(t) f(t) \right] \right\} dt. \end{aligned} \tag{7}$$

where λ, β_1 and β_2 are the Lagrange multipliers associated with the dynamical state equation for $x(t)$ and the constraints on the control signal $f(t)$, while the slack variables ξ_1 and ξ_2 are needed to convert the inequality bounds on $f(t)$ into equality constraints.

By expanding L around $\tau = 0$, using Taylor series expansion and setting $\frac{\partial L}{\partial \tau} = 0$, we get:

$$\frac{\partial L}{\partial x} + {}_t D_{t_f}^{\alpha} \frac{\partial L}{\partial_{t_i} D_t^{\alpha} x} = 0, \quad \frac{\partial L}{\partial f} = 0, \quad \frac{\partial L}{\partial \lambda} = 0, \quad \frac{\partial L}{\partial \beta_1} = 0, \quad \frac{\partial L}{\partial \beta_2} = 0 \tag{8}$$

where ${}_t D_{t_f}^{\alpha}$ and ${}_{t_i} D_t^{\alpha}$ represent fractional derivatives operating forward and backward in time, respectively.

In order to solve Equation (8), we discretize the interval $[t_i, t_f]$ into N equal intervals of size $\Delta t = \frac{(t_f - t_i)}{N}$. The formula in Equation (2) can be used to express the optimality conditions as follows:

$$\sum_{i=0}^{k} \frac{(-1)^i}{\Delta t^{\alpha}} \binom{\alpha}{i} x((k-i)\Delta t) - a(k\Delta t)x(k\Delta t) + \frac{(b(k\Delta t))^2 [\lambda(k\Delta t) + \beta_1(k\Delta t) - \beta_2(k\Delta t)]}{z(k\Delta t)} = 0, \tag{9}$$

where $k = 1, \ldots, N$ represents the k-th discretization time interval,

$$\begin{aligned} &\sum_{i=0}^{N-k} \frac{(-1)^i}{\Delta t^{\alpha}} \binom{\alpha}{i} \lambda((k+i)\Delta t) - w(k\Delta t)[x(k\Delta t) - x_{ref}] \\ &- a(k\Delta t)\lambda(k\Delta t) - \frac{\lambda(N\Delta t)(t_f - t_i - k\Delta t)^{-\alpha}}{\Gamma(1-\alpha)} = 0, \end{aligned} \tag{10}$$

where $k = N-1, \ldots, 0$

$$\frac{\beta_2(k\Delta t) - \beta_1(k\Delta t) - b(k\Delta t)\lambda(k\Delta t)}{z(k\Delta t)} - \xi_1(k\Delta t) = f_{min} \qquad k = 1, \ldots, N \tag{11}$$

$$\frac{\beta_2(k\Delta t) - \beta_1(k\Delta t) - b(k\Delta t)\lambda(k\Delta t)}{z(k\Delta t)} + \xi_2(k\Delta t) = f_{max} \qquad k = 1, \ldots, N. \tag{12}$$

At this stage, we are able to convert the problem defined by equations (3) to (6) into solving the discrete time equations described from (9) to (12), which can reduce to either solving a linear system when no inequality constraints are considered or a linear program when tight bounds on both the state and control variables are considered.

4.2. Finite Time Fractal Optimal Control with Integral of Absolute Value of Tracking Error Criterion (IAE)

The cost function that needs to be minimized in this case is as follows:

$$\min_{f(t)} \frac{1}{2} \int_{t_i}^{t_f} [w(t)|x(t) - x_{ref}| + z(t)f(t)^2]dt \tag{13}$$

subject to constraints given by Equations (4), (5), and (6), respectively.

By focusing on the absolute value of the error in Equation (13), the optimal controller tries to find the pacing frequency such that positive and negative deviations from the reference value for the R-R interval are minimized. This criterion is more sensitive to parameter variations when compared to the squared error criterion. Also, using the absolute difference of error evaluates to linear equations when finding optimality conditions is easier to implement in practice. The simplicity of this cost function makes it very suitable for computer simulations.

To solve this optimal control problem, we use again the concept of Lagrange multipliers as follows:

$$L(x,\ f, w, z, \beta_1, \xi_1, \beta_2, \xi_2, \lambda) = \int_{t_i}^{t_f} \left\{ \frac{w(t)|x(t) - x_{ref}|}{2} + \frac{z(t) f(t)^2}{2} + \beta_1(f - f_{min} - \xi_1) + \beta_2(f_{max} - f - \xi_2) - \lambda \left[\frac{d^\alpha x(t)}{dt^\alpha} - a(t)x(t) - b(t) f(t) \right] \right\} dt. \tag{14}$$

where λ, β_1, β_2, ξ_1 and ξ_2 have the same meanings as the Lagrange multipliers in Equation (7).

Applying the optimality conditions as defined by the ones in Equation 8 on the new Lagrangian function L given in Equation (14), we get the following relations together with the conditions defined by Equations (9), (11) and (12), respectively:

$$\sum_{i=0}^{N-k} \frac{(-1)^i}{\Delta t^\alpha} \binom{\alpha}{i} \lambda((k+i)\Delta t) - \frac{w(k\Delta t)}{2} sgn(x(k\Delta t) - x_{ref}) - a(k\Delta t)\lambda(k\Delta t) - \frac{\lambda(N\Delta t)(t_f - t_i - k\Delta t)^{-\alpha}}{\Gamma(1-\alpha)} = 0, \tag{15}$$

where $k = N-1, \ldots, 0$ and $sgn(x)$ is defined as:

$$\begin{aligned} sgn(x) &= \ \ 1 \quad if \quad x > 0 \\ &= -1 \quad if \quad x < 0. \end{aligned}$$

4.3. Finite Time Fractal Optimal Control with Integral of Time Multiplied by Absolute Error Criterion (ITAE)

The cost function that needs to be minimized in this case is as follows:

$$\min_{f(t)} \frac{1}{2} \int_{t_i}^{t_f} [t\ w(t)\ |x(t) - x_{ref}| + z(t) f(t)^2] dt \tag{16}$$

subject to constraints given by Equations (4), (5), and (6), respectively.

The absolute error minimization criterion discussed in the previous section has a drawback, namely it can produce large overshoots and oscillations of $x(t)$. Also, the time at which the values of $x(t)$ become close to x_{ref} may play in some medical conditions a crucial role.

The criterion introduced in Equation (16) is much more selective than the previous two cost functions summarized in Equation (3) and (13), respectively. Therefore, by focusing on the integral of the absolute value of error multiplied by the time at which this error occurs, as shown in Equation (16), the optimal controller tries to find the pacing frequency such that positive and negative deviations from the reference value for the R-R interval, as well as the time at which it occurs are minimized. The criterion used here weights the existing error $(x(t) - x_{ref})$ more heavily after long times as opposed to those existing initially. Also, using this criterion gives small overshoots and oscillations. However, this cost function is more sensitive to parameter variations as compared to the other two discussed above.

To solve this optimal control problem, we use again the concept of Lagrange multipliers as follows:

$$L(x,\ f, w, z, \beta_1, \xi_1, \beta_2, \xi_2, \lambda) = \int_{t_i}^{t_f} \left\{ \frac{t\ w(t)\ |x(t) - x_{ref}|}{2} + \frac{z(t)f(t)^2}{2} + \beta_1(f - f_{min} - \xi_1) + \beta_2(f_{max} - f - \xi_2) - \lambda\left[\frac{d^\alpha x(t)}{dt^\alpha} - a(t)x(t) - b(t)f(t)\right]\right\} dt. \tag{17}$$

where λ, β_1, β_2, ξ_1 and ξ_2 have the same meanings as the Lagrange multipliers in Equation (7).

Applying the optimality conditions as defined by the ones in Equation (8) on the new Lagrangian function L given in Equation (17), we get the following relations together with the conditions defined by Equations (9), (11), and (12), respectively:

$$\sum_{i=0}^{N-k} \frac{(-1)^i}{\Delta t^\alpha}\binom{\alpha}{i}\lambda((k+i)\Delta t) - \frac{w(k\Delta t)(k\Delta t)}{2} sgn(x(k\Delta t) - x_{ref}) - a(k\Delta t)\lambda(k\Delta t) - \frac{\lambda(N\Delta t)(t_f - t_i - k\Delta t)^{-\alpha}}{\Gamma(1-\alpha)} = 0 \tag{18}$$

for all $k = N-1, \ldots, 0$.

4.4. Finite Time Fractal Optimal Control with Integral of Time Multiplied by Squared Tracking Error Criterion (ITSE)

The cost function that needs to be minimized in this case is as follows:

$$\min_{f(t)} \frac{1}{2}\int_{t_i}^{t_f} [t\ w(t)\ (x(t) - x_{ref})^2 + z(t)f(t)^2]dt \tag{19}$$

subject to constraints given by Equations (4), (5), and (6), respectively.

By focusing on the integral of the square of error multiplied by time in Equation (19), the optimal controller tries to find the pacing frequency such that positive and negative deviations from the reference value for the R-R interval, as well as the time at which they occur are minimized. Overshoots and oscillations produced are also smaller in this case. However, the controller is less sensitive to parameter variations as compared to time multiplied by absolute error criterion.

To solve this optimal control problem, we use again the concept of Lagrange multipliers as follows:

$$L(x,\ f, w, z, \beta_1, \xi_1, \beta_2, \xi_2, \lambda) = \int_{t_i}^{t_f} \left\{ \frac{t\ w(t)\ (x(t) - x_{ref})^2}{2} + \frac{z(t)f(t)^2}{2} + \beta_1(f - f_{min} - \xi_1) + \beta_2(f_{max} - f - \xi_2) - \lambda\left[\frac{d^\alpha x(t)}{dt^\alpha} - a(t)x(t) - b(t)f(t)\right] dt \right\} \tag{20}$$

where λ, β_1, β_2, ξ_1 and ξ_2 have the same meanings as the Lagrange multipliers in Equation (7).

Applying the optimality conditions as defined by the ones in Equation (8) on the new Lagrangian function L given in Equation (20), we get the following relations together with the conditions defined by Equations (9), (11), and (12), respectively:

$$\sum_{i=0}^{N-k} \frac{(-1)^i}{\Delta t^\alpha} \binom{\alpha}{i} \lambda((k+i)\Delta t) - w(k\Delta t)\,(k\Delta t)\,[x(k\Delta t) - x_{ref}] \\ - a(k\Delta t)\lambda(k\Delta t) - \frac{\lambda(N\Delta t)(t_f - t_i - k\Delta t)^{-\alpha}}{\Gamma(1-\alpha)} = 0 \tag{21}$$

for all $k = N-1, \ldots, 0$.

4.5. Finite Time Fractal Optimal Control with Integral of Squared Time Multiplied by Squared Tracking Error Criterion (ISTSE)

The cost function that needs to be minimized in this case is as follows:

$$\min_{f(t)} \frac{1}{2} \int_{t_i}^{t_f} [t^2\ w(t)\,(x(t) - x_{ref})^2 + z(t)f(t)^2]dt \tag{22}$$

subject to constraints given by Equations (4), (5), and (6), respectively.

By focusing on the integral of the square of error multiplied by square of the time at which this error occurs, as given in Equation (22), we synthesize a controller that avoids large errors as time passes; this is because the errors that exist after long times are weighed more heavily as compared to the cost function in Section 4.4.

To solve this optimal control problem, we use again the concept of Lagrange multipliers as follows:

$$L(x,\,f,w,z,\beta_1,\xi_1,\beta_2,\xi_2,\lambda) = \int_{t_i}^{t_f} \left\{ \frac{t^2\ w(t)\,(x(t)-x_{ref})^2}{2} + \frac{z(t)f(t)^2}{2} + \beta_1(f - f_{min} - \xi_1) \right. \\ \left. + \beta_2(f_{max} - f - \xi_2) - \lambda\left[\frac{d^\alpha x(t)}{dt^\alpha} - a(t)x(t) - b(t)f(t)\right]\right\} dt. \tag{23}$$

where λ, β_1, β_2, ξ_1 and ξ_2 have the same meanings as the Lagrange multipliers in Equation (7).

Applying the optimality conditions as defined by the ones in Equation (8) on the new Lagrangian function L given in Equation (23), we get the following relations together with the conditions defined by Equations (9), (11) and (12), respectively:

$$\sum_{i=0}^{N-k} \frac{(-1)^i}{\Delta t^\alpha} \binom{\alpha}{i} \lambda((k+i)\Delta t) - w(k\Delta t)\,(k\Delta t)^2\,[x(k\Delta t) - x_{ref}] \\ - a(k\Delta t)\lambda(k\Delta t) - \frac{\lambda(N\Delta t)(t_f - t_i - k\Delta t)^{-\alpha}}{\Gamma(1-\alpha)} = 0 \tag{24}$$

for all $k = N-1, \ldots, 0$.

4.6. Finite Time Fractal Optimal Control with Integral of Fourth Power of Time Multiplied by Squared Tracking Error Criterion

The cost function that needs to be minimized in this case is as follows:

$$\min_{f(t)} \frac{1}{2} \int_{t_i}^{t_f} [t^4\ w(t)\,(x(t) - x_{ref})^2 + z(t)f(t)^2]dt \tag{25}$$

subject to constraints given by Equations (4), (5) and (6), respectively.

Table I.
Estimated parameters for non-fractal (i.e., 1-step ARMA) and fractal model for 5 different time series of R-R interval for healthy individuals [PhysioNet]. Comparison between a non-fractal model and a fractal model in terms the goodness-of-fit is also tabulated. All time series except for those with ID 3 have a *p-value* of 1 which suggests that the fractal model should be used to model heart rate activity.

Heart rate	Classical (non-fractal) model				Fractal model				
	Parameters of the Model		Goodness-of-fit		Parameters of the Model			Goodness-of-fit	
Time series ID	a	b	p-value	Test statistic	α	a	b	p-value	Test statistic
1	0.9665	0.0267	0	61.127	0.6226	0.1613	−0.1284	1	0.2754
2	0.979	0.0193	0	30.031	0.7762	0.0355	−0.0326	1	0.2564
3	0.9513	0.0403	0	120.880	0.707	0.1255	−0.1038	0.51	0.3182
4	0.9525	0.0409	0	73.945	0.7258	0.1105	−0.0951	1	0.2544
5	0.9663	0.0286	0	88.339	0.699	0.0643	−0.0546	1	0.2714

To solve this optimal control problem, we use again the concept of Lagrange multipliers as follows:

$$L(x,\ f, w, z, \beta_1, \xi_1, \beta_2, \xi_2, \lambda) = \int_{t_i}^{t_f} \left\{ \frac{w(t)\, t^4\, (x(t) - x_{ref})^2}{2} + \frac{z(t) f(t)^2}{2} + \beta_1(f - f_{min} - \xi_1) + \beta_2(f_{max} - f - \xi_2) - \lambda \left[\frac{d^\alpha x(t)}{dt^\alpha} - a(t)x(t) - b(t) f(t) \right] \right\} dt. \tag{26}$$

where λ, β_1, β_2, ξ_1 and ξ_2 have the same meanings as the Lagrange multipliers in Equation (7).

Applying the optimality conditions as defined by the ones in Equation (8) on the new Lagrangian function L given in Equation (26), we get the following relations together with the conditions defined by Equations (9), (11) and (12), respectively:

$$\sum_{i=0}^{N-k} \frac{(-1)^i}{\Delta t^\alpha} \binom{\alpha}{i} \lambda((k+i)\Delta t) - w(k\Delta t)\, (k\Delta t)^4\, [x(k\Delta t) - x_{ref}] - a(k\Delta t)\lambda(k\Delta t) - \frac{\lambda(N\Delta t)(t_f - t_i - k\Delta t)^{-\alpha}}{\Gamma(1-\alpha)} = 0 \tag{27}$$

for all $k = N-1, \ldots, 0$.

5. EXPERIMENTAL SETUP AND RESULTS

The optimal control approaches introduced in Section 4 make sense only if the predicted model of heart is appropriate. Therefore, we first estimate the heart parameters using fractal and non-fractal approaches and then compute the goodness-of-fit for each model. We perform a hypothesis testing to verify whether the observed data can be modeled by each specific model. The observed *p-value* is a measure of closeness between the proposed model and the actual data. Next, we provide a complete experimental analysis of the problems introduced in Section 4.

5.1. Parameter Identification of Fractional Calculus Model

Using real world heart rate time series from PhysioNet, we compute the parameters of the heart rate activity model by using two approaches: i) Using ordinary differential

Table II.
Estimated parameters for non-fractal (i.e., 1-step ARMA) and fractal model for 5 different time series of R-R interval for patients with atrial fibrillation [PhysioNet]. Comparison between a non-fractal model and a fractal model in terms the goodness-of-fit is also tabulated. Fractional order differential equation can be used to model the heart rate of patient with atrial fibrillation as justified by the *p-value*.

Heart rate	Classical (non-fractal) model				Fractal model				
	Parameters of the Model		Goodness-of-fit		Parameters of the Model			Goodness-of-fit	
Time series ID	a	b	p-value	Test statistic	α	a	b	p-value	Test statistic
1	0.0407	−0.0245	0.0018	0.3845	0.6597	0.5827	0.3508	0.8471	0.295
2	0.0007	−0.0005	0.0031	0.3806	0.6841	0.7302	0.5853	0.4296	0.3224
3	0.0050	0.0055	0.0036	0.3795	0.6371	0.7862	0.8697	0.5523	0.3153
4	0.0289	0.0167	0.0017	0.3851	0.6307	0.8082	0.4659	0.226	0.3354
5	−0.0225	0.0142	0.0144	0.3681	0.6516	0.6850	0.4316	0.5098	0.3178

equation of order 1 and computing a and b (i.e., in Equation (4)) and ii) Using fractional differential equation and computing a , b and α coefficients in Equation (4).

To discriminate between the suitability of modeling the heart rate time series via either an integer or a fractional order differential equation, we use the periodogram method developed by Beran [1994], which relies on estimating the moments of the observations, comparing them with those of the postulated models, and finally evaluate the goodness-of-fit so we can compare the accuracy of the two models. The goodness-of-fit is calculated at a threshold of 0.05, which is usually a reasonably good statistical significance level. This means that if the *p-value* calculated is less than 0.05, then with 95% confidence, we can reject the goodness of that particular model.

By estimating the parameters of the model via maximum likelihood method, computing the goodness-of-fit results and comparing the 4th and 9th columns of Table I, we can draw the following conclusions.

—Modeling the heart rate via classical (i.e., integer or non-fractal) model has to be rejected because of getting a *p-value* equal to 0.
—Modeling via fractional differential equation cannot be rejected and should be preferred over classical first order ordinary differential equations.

The parameters predicted and their goodness-of-fit are depicted in Table I.

5.2. Performance Analysis of Constrained Finite Horizon Optimal Control Problem

In order to analyze the performance of the control problem for the six cost functions mentioned in Section 4 along with the given constraints, we consider a time series of a patient suffering from bradycardia [PhysioNet]. Under this condition, the heart rate is typically below 60 beats per minute; this may result in cardiac arrest because of insufficient pumping of oxygen by heart, fainting, shortness of breath, and in some cases even death.

The R-R interval corresponding to 60 beats per minute is 1s. The normal heart rate is 75 beats per minute, which corresponds to an R-R interval of 0.8 seconds. Therefore the objective of the control problem is to bring the R-R interval down for a patient suffering from bradycardia to the normal level of 0.8 seconds. In Table II, we calculate the parameters and goodness-of-fit for patients suffering with atrial fibrillation. It can be observed that although the *p-value* for the classical case is greater than 0, it still remains below the statistically significant level. Also, the *p-value* for the fractal model

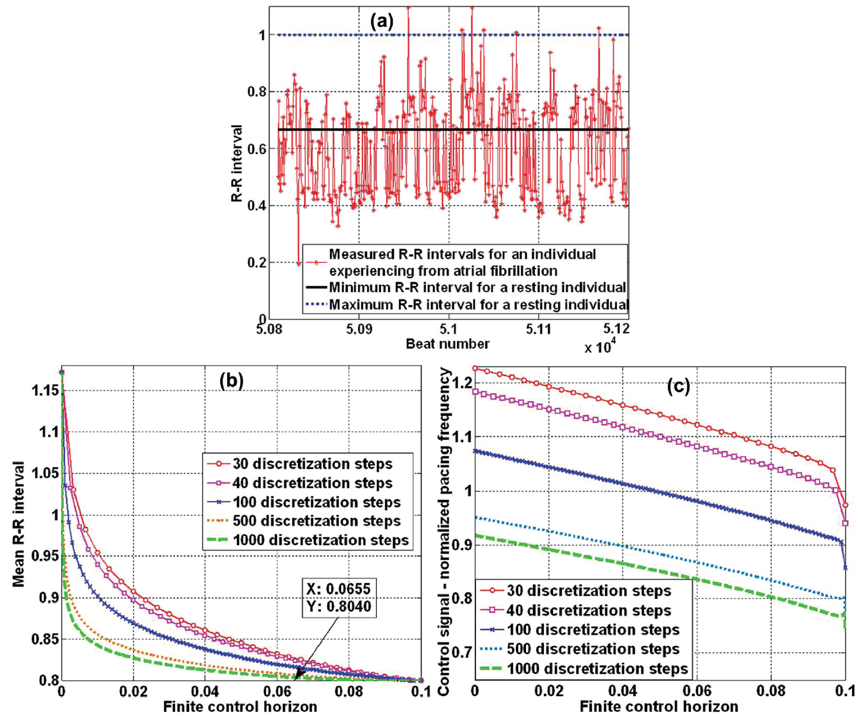

Fig. 5. (a) Comparison between the measured R-R intervals of a patient suffering from bradycardia and the minimum and maximum bounds on the measured R-R intervals for a healthy individual at rest. It can be clearly seen that the R-R interval values are on the higher side. The average R-R interval value for the first 100 beats is 1.1 seconds. The standard deviation is 0.27 seconds. This can lead to cardiac arrest, faintness, shortness of breath. In addition, one can note that the controller exhibits less than 1% error after only 66% of the finite control horizon. (b) Applied fractal optimal controller with mean squared error criterion which decreases the R-R interval to 0.8 seconds in 0.1 seconds. (c) Normalized pacing frequency that results in increasing the heart rate from approximately 50 beats per minute to 75 beats per minute.

is significant; this implies that the fractal model cannot be rejected for patients with atrial fibrillation.

The first step in our experiment is to analyze the goodness-of-fit for both the models, i.e., non-fractal and fractal model. The time series with ID3 in Table II come from a patient suffering from bradycardia. As it can be seen from this table, the p-value for the non-fractal model is only 0.0036, which is below the significance level of 0.05; hence the non-fractal model cannot be applied. However, the fractal model has a p-value of 0.5523, which is well above the significance level; hence we can apply this fractal model to solve the finite time control problem.

After analysing the goodness-of-fit and deciding which model to use, the next step is to solve the control problem using the appropriate model of the heart. The control problem aims at finding out the optimal pacing frequency such that the heart rate of 75 beats per minute is achieved within a finite time horizon of 0.1 seconds. The results for the values of controlled R-R interval and the pacing frequency are shown in Figures 5 to 10, respectively, for the optimal control problem as mentioned in Sections 4.1 to 4.6, respectively.

The w and z coefficients for the finite time optimal control problem (as mentioned in Section 4.1) are chosen to be both 1. As it can be seen in Figure 5(b), within a finite time horizon of 0.1 seconds, the desired value for the R-R interval, which is 0.8 (equivalent to 75 beats per minute) is achieved for all discretization steps (i.e.,

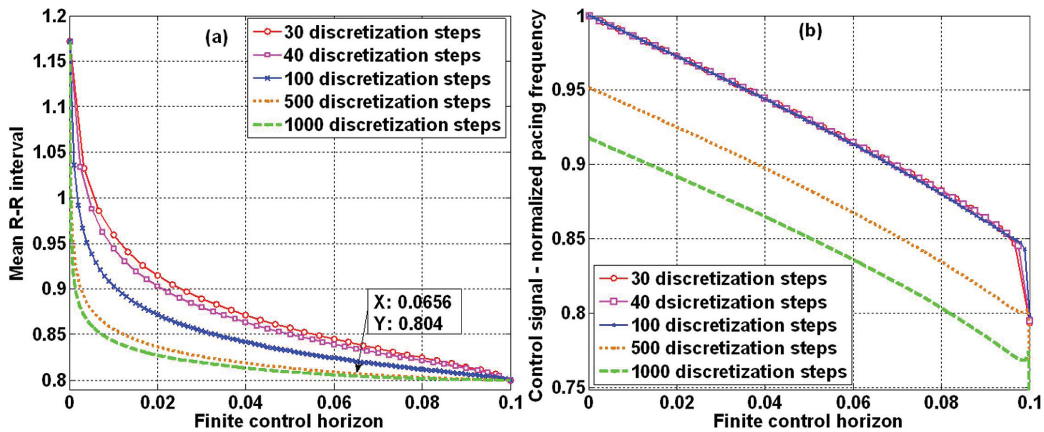

Fig. 6. (a) Applying the fractal optimal controller described in Section 4.2; as shown, the R-R interval is decreased from 1.2 seconds to 0.8 seconds in a finite time horizon of 0.1 seconds. (b) Controlled normalized pacing frequency required by the control problem described in Section 4.2 to increase the heart rate to 75 beats per minute.

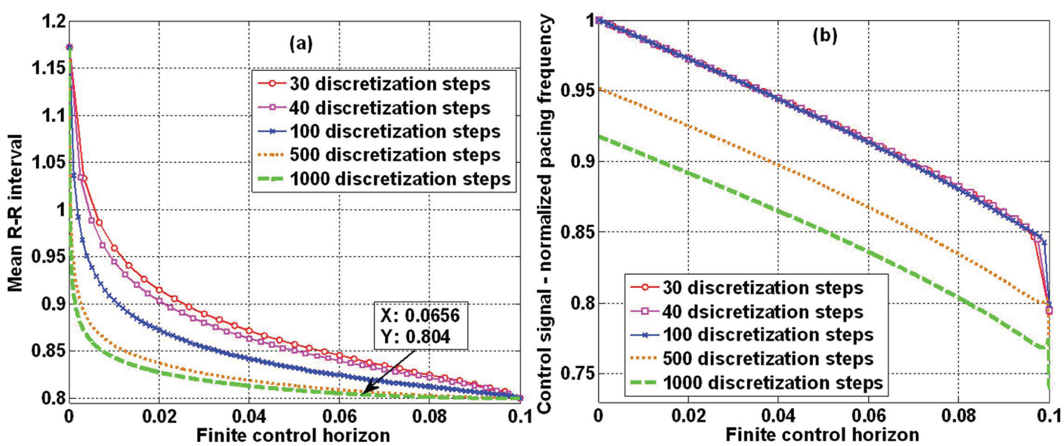

Fig. 7. (a) Applying the fractal optimal controller described in Section 4.3; as shown, the R-R interval is decreased from 1.2 seconds to 0.8 seconds in a finite time horizon of 0.1 seconds. (b) Controlled normalized pacing frequency required by control problem described in Section 4.3 to increase the heart rate to 75 beats per minute.

$N = 30, 40, 100, 500$ *and* 1000). Figure 5(c) shows the control signal pacing frequency, which varies as a function of time. The final normalized control pacing frequency when $N = 30, 40, 100$ *or* 500 discretization steps are considered, turns out to be 0.8021; for $N = 1000$ it is 0.7738 Consequently, the loss in accuracy for computing the control pacing frequency from fewer discretization steps ($N = 30, 40$ *and* 100) compared to using a greater number of discretization steps ($N = 1000$) is only 5.7%.

The effect of the cost function on the mean R-R interval and normalized pacing frequency is not significant; this can be seen in Figures 5(b), 5(c), 6(a), 6(b), 7(a), 7(b), 8(a), 8(b), 9(a), 9(b), 10(a) and 10(b). In all these cases, the desired normal R-R interval of 0.8 seconds is attained. Within a time horizon of 0.0656 seconds, the R-R interval value reaches a value of 0.804 seconds, which is within 0.5% (i.e., $y = 1$) of the desired R-R value.

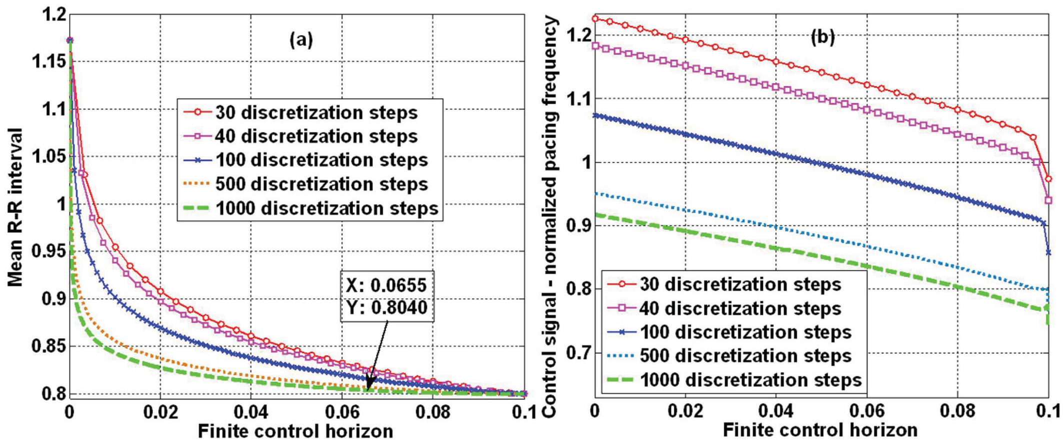

Fig. 8. (a) Applying the fractal optimal controller described in subsection 4.4; as shown, the R-R interval is decreased from 1.2 seconds to 0.8 seconds in a finite time horizon of 0.1 seconds. (b) Controlled normalized pacing frequency required by control problem described in subsection 4.4 to increase the heart rate to 75 beats per minute.

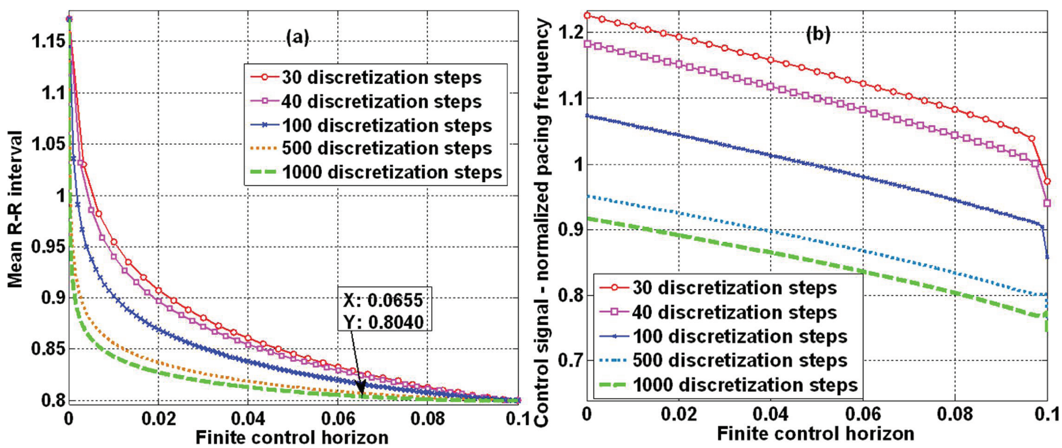

Fig. 9. (a) Applying the fractal optimal controller described in subsection 4.5; the R-R interval is decreased from 1.2 seconds to 0.8 seconds in a finite time horizon of 0.1 seconds. (b) Controlled normalized pacing frequency required by control problem described in subsection 4.5 to increase the heart rate to 75 beats per minute.

Next, we consider the effect of changing the value of the weighting coefficient w when solving the optimal control problems described in Section 4.1 and Section 4.2. This is shown in Figures 11 and 12, respectively.

In Figure 11, one can observe that changes in the w value do not change the convergence characteristics significantly, which means that the squared error term is more dominant as compared to the weighting coefficient in determining the convergence time. In Figure 12, however, the red curve for $w = 5$ dips faster as compared to the other curves; this means that, in the absolute error case, the effect of weighting coefficient is more significant than that in the squared error case.

The results given in this section suggest that in a finite time horizon of 0.1 seconds, the reference value of the R-R interval (i.e., 0.8 seconds) can be achieved using any of the cost function described in Section 4. Also, the squared error criterion converges

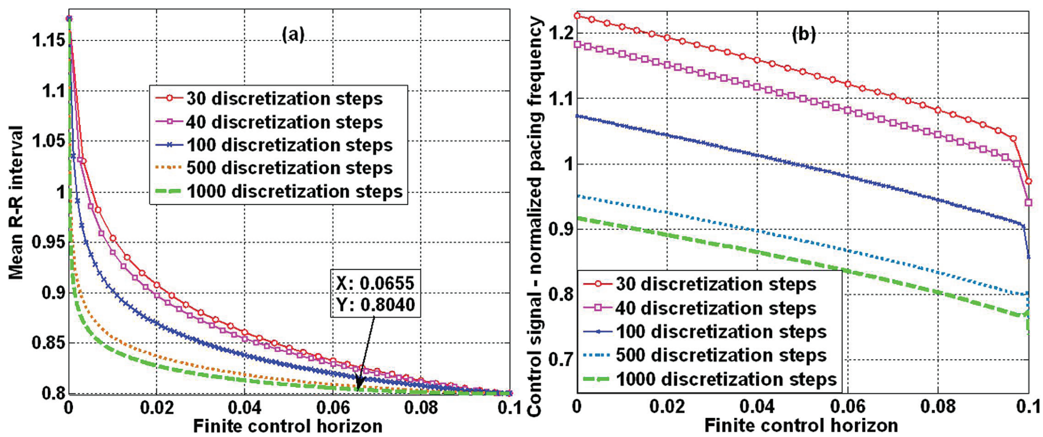

Fig. 10. (a) Applying the fractal optimal controller described in Section 4.6; the R-R interval is decreased from 1.2 seconds to 0.8 seconds in a finite time horizon of 0.1 seconds. (b) Controlled normalized pacing frequency required by control problem described in Section 4.6 to increase the heart rate to 75 beats per minute.

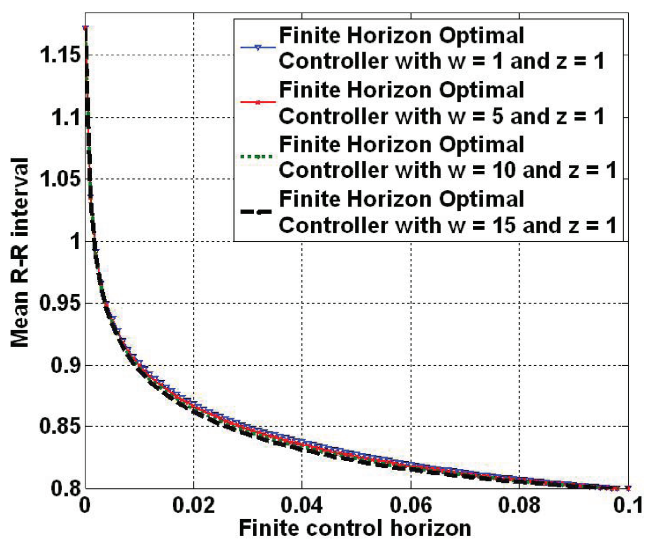

Fig. 11. Effect of changes in the w value on the convergence characteristics for optimal control problem described in Section 4.1.

faster than the absolute error criterion. The effect of changing the value of weighting coefficient w is more significant when considering the absolute error criterion as compared to squared error one.

5.3. Hardware Complexity of Fractal Optimal Controller

The *Observation* module in Figure 2 refers to some digital filters required to estimate the parameters of the model either in the frequency or wavelet domains. The *Actuation* module in Figure 2 refers to a series of electrodes that can deliver to the heart specific control signals (i.e., electrical pulses of predefined amplitude and duration) to cause the depolarization of the myocardium. Consequently, we consider next the hardware complexity of the controller as this contributes the most to the overall CPS design.

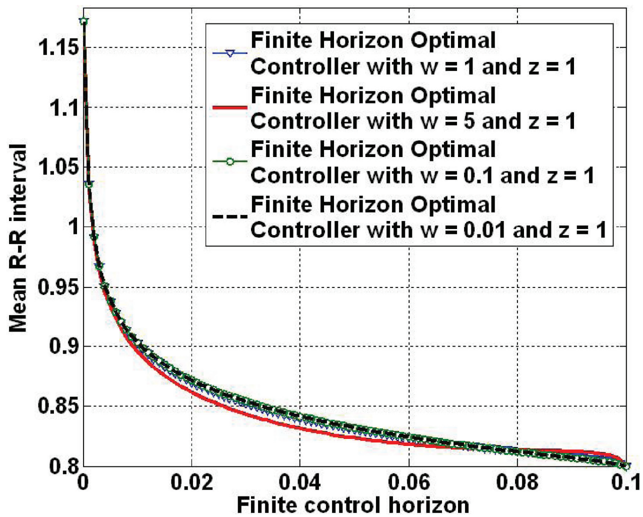

Fig. 12. Effect of changes in the w value on the convergence characteristics for optimal control problem described in Section 4.2.

In Section 4, we have presented the formulation of fractal optimal control problem and provided a discrete time linearization of the same. The discrete time linearization can be interpreted as a linear matrix equation of the form $Ax = B$, where A is a $2N \times 2N$ matrix and B is a $2N \times 1$ column vector, x is a $2N \times 1$ column vector solution to this equation. In this section, the hardware complexity (i.e., area overhead) is investigated for implementation of the fractal optimal controller through an FPGA prototype.

There are several ways to solve the linear matrix equation such as: Gaussian elimination, LU factorization, Cramer's method and iterative methods. The time complexity associated with Gaussian elimination and LU factorization is $O(N^3)$ where N is the number of unknown variables. Better time complexity in solving the linear matrix equation can be achieved by using the Cramer's method if parallel processing elements are used. This is discussed next.

The time complexity of Cramer's method for solving the linear matrix equation is based on the efficiency in calculating the determinant of an $N \times N$ matrix. Determinant calculation can be done in $O(N)$ time using Chio's pivotal condensation process by making use of $(N-1)^2$ parallel processing elements [Sridhar et al. 1987]. In Chio's pivotal condensation process an initial matrix of order $N \times N$ is iteratively reduced to a matrix of order 2×2. In each iteration the matrix is reduced by order 1. So the reduction operation requires $O(N)$ time.

At each reduction step, $O(N^2)$ 2×2 determinants are calculated. So if we have $(N-1)^2$ parallel processing elements, the entire determinant calculation can be done in $O(N)$ time. These processing elements are multiply and accumulate (MAC) units. Hence performance can be increased at an additional cost of an added MAC unit.

We have implemented this on a Xilinx Virtex4 FPGA (Device: $XC5VLX30$ and Package: $FF324$). Xilinx SXT is used for synthesis and the ISim package is used for simulations [Xilinx].

Table III summarizes the area overhead of the designed controller in terms of the slice, LUT, and register utilization. The worst case time to solve a 16×16 determinant using only one Chio's Pivotal Condensation processing element is 1190 clock cycles. Here DSP 48 refers to the Digital Signal Processing slice [XilinxDSP].

Table III. Controller area Consumption in Terms of the Number of Slices, Registers, LUTs

Size of Linear System	Registers	LUT	RAM/FIFO	DSP48s
16	243	239	1	6
128	340	618	29	6

6. CONCLUSION

In this article, we have discussed several approaches for pacemaker design needed to control the heart rate variability as a fundamental CPS optimization problem. Towards this end, we have solved a constrained finite horizon fractal optimal control approach to regulate R-R interval and analyzed the goodness-of-fit of fractal model to R-R dynamics. In addition, the comparison of goodness-of-fit with the classical (non-fractal) model was also discussed. Then, using the fractal model of heart, the controller was designed for six different cost functions and their performance for patient suffering from bradycardia was analyzed as a concrete example. Finally, the feasibility of building this CPS was analyzed by reporting the area overhead values obtained from FPGA implementation.

As future work, we plan to investigate the stability of the controller in presence of uncertainties and analyze the performance of various cost functions that make use of higher order moments.

ACKNOWLEDGMENTS

The authors would like to thank the anonymous reviewers for their constructive comments and helpful suggestions.

REFERENCES

Agrawal, O. P., Defterli, O., and Baleanu, D. 2010. Fractional optimal control problems with several state and control variables. *Vibration Control 16,* 13, 1967–1976.

Alt, E., Matula, M., and Theres, H. 1989. The basis for activity controlled rate variable cardiac pacemakers: an analysis of mechanical forces on the human body induced by exercise and environment. *Pacing Clin. Electrophysiol. 12,* 10, 1667–1680.

Bacharach, D. W., Hilden, T. S., Millerhagen, J. O., Westrumand, B. L., and Kelly, J. M. 1992. Activity-based pacing: comparison of a device using an accelerometer versus a piezoelectric crystal. *Pacing Clin Electrophysiol. 15,* 2, 188–196.

Battaglia, J. L., Lay, L. L., Batsale, J.-C., Oustaloup, A., and Cois, O. 2000. Heat flow estimation through inverted non integer identification models. *J. Thermal Sciences 39,* 3, 374–389.

Beran, J. 1994. *Statistics for Long-Memory Processes*. Chapman and Hall.

Bogdan, P., Jain, S., Goyal, K., and Marculescu, R. 2012. Implantable pacemakers control and optimization via fractional calculus approaches: A cyber physical systems perspective. In *Proceedings of the 3rd ACM/IEEE International Conference on Cyber Physical Systems(ICCPS'12)*. ACM, 23–32.

Bogdan, P. and Marculescu, R. 2011. Towards a science of cyber physical system design. In *Proceedings of the 2nd ACM/IEEE International Conference on Cyber Physical Systems (ICCPS'11)*. ACM, 99–108.

Coenan, M., Malinowski, K., Spitzer, W., Schuchert, A., Schmitz, D., Anelli-Monti, M., Maier, S. K., Estlinbaum, W., Bauer, A., Muehling, H., Kalscheur, F., Puerner, K., Boergel, J., and Osswald, S. 2008. Closed loop stimulation and accelerometer-based rate adaptation: Results of the provide study. *Europace 10,* 3, 327–333.

Dell'orto, S., Valli, P., and Greco, E. M. 2004. Sensors for rate responsive pacing. *Indian Pacing Electrophysio. J. 4,* 3, 137–145.

Doyle-III, F. J., Bequette, B. W., Middleton, R., Ogunnaike, B., Paden, B., Parker, R. S., and Vidyasagar, M. 2011. Control in biological systems. http://ieeecss.org/sites/ieeecss.org/files/documents/IoCT-Part1-05ControlBioSystems.pdf.

Fauci, A. S., Braunwald, E., Hauser, S. L., Longo, D. L., Jameson, J., and Loscalzo, J. 2008. *Harrison's Principles of Internal Medicine*. Mc-Graw Hill.

Graham, D. and Lathrop, R. C. 1953. The synthesis of optimum transient response: Criteria and standard forms. *AIEE Trans. 273,* 72.

HADDAD, S. A. P., HOUBEN, R. P. M., AND SERDIJN, W. A. 2006. The evolution of pacemakers. *IEEE Eng. Medicine Bio. 25,* 3, 38–48.

HEXAMER, M. P. R., MEINE, M., KLOPPE, A., AND WERNER, E. 2001. Rate-responsive pacing based on the atrio-ventricular conduction time. *IEEE Trans. Biomed. Eng. 49,* 3, 185–195.

HUMEN, D. P., KOSTUK, W. J., AND KLEIN, G. J. 1985. Activity-sensing,rate-responsive pacing: Improvement in myocardial performance with exercise. *Pacing Clin. Electrophysiol. 8,* 1, 52–59.

HUNG, G. K. 1990. Application of the root locus technique to the closed loop SO_2 pacemaker-cardiovascular system. *IEEE Trans. BioMed. Eng. 37,* 6, 549–555.

INBAR, G. F., HEINZE, R., HOEKSTEIN, K. N., LIESS, H. D., STANGL, K., AND WIRTZFELD, A. 1988. Development of a closed-loop pacemaker controller regulating mixed venous oxygen saturation level. *IEEE Trans. BioMed. Eng. 35,* 9, 679–690.

IVANOV, P. C., AMARAL, L. A. N., GOLDBERGER, A. L., HAVLIN, S., ROSENBLUM, M. G., STANLEY, H. E., AND STRUZIK, Z. R. 2001. From 1/f noise to multifractal cascades in heartbeat dynamics. *Chaos 11,* 3, 641–652.

IVANOV, P. C., BUNDE, A., AMARAL, L. A. N., HAVLIN, S. J., FRITSCH-YELLE, BAEVSKY, R. M., STANLEY, H. E., AND GOLDBERGER, A. E. 1999. Sleep-wake differences in scaling behavior of the human heart-beat: Analysis of terrestrial and long-term space flight data. *Europhys. Lett. 48,* 5, 594–600.

IVANOV, P. C., ROSENBLUM, M. G., K-PENG, C., MIETUS, J., HAVLIN, S., STANLEY, H. E., AND GOLDBERGER, A. L. 1998. Scaling and universality in heart rate variability distributions. In *Proceedings of Bar-Ilan Conference Physica A 249,*. 587–593.

JAEGAR, F. J. 2010. Disease management project, cardiology, cardiac arrhythmias, cleaveland clinic. http://www.cleavelandclinicmeded.com/medicalpubs/diseasemanagemaent/cardiology/cardiac-arrhythmias.

JIANG, Z., PAJIC, M., AND MANGHARAM, R. 2011. Model-based closed-loop testing of implantable pacemakers. In *Proceedings of the 2nd ACM/IEEE International Conference on Cyber Physical Systems (ICCPS'11)*. ACM, 131–140.

KIYONO, K., YAMAMOTO, Y., AND STRUZIK, Z. R. 2009. *Statistical Physics of Human Heart Rate in Health and Disease in Understanding Complex Systems*. Springer.

LEE, E. A. 2010. Cps foundations. In *Proceedings of the 47th ACM/IEEE Design Automation Conference (DAC '10)*. ACM, 737–742.

LEE, S. Y., CHENG, C. J., AND LIANG, M. C. 2011. A low-power bidirectional telemetry device with a near-field charging feature for a cardiac microstimulator. *IEEE Trans. Biom. Circ. Syst. 5,* 4, 357–367.

LI, N., CRUZ, J., CHIEN, C., SOJOUDI, S., RECHT, B., STONE, D., CSETE, M., BAHMILLER, D., AND DOYLE, J. C. 2012. Robust efficiency and actuator saturation explain healthy heart rate variability. To appear.

LOPEZ, M. J., CONSEGLIERE, A., LORENZO, J., AND GARCIA, L. 2010. Computer simulation and method for heart rhythm control based on ecg signal reference tracking. *WSEAS Trans. Syst. 9,* 1, 263–272.

MAGIN, R. L. 2006. *Fractional Calculus in Bioengineering*. Begell House Publishers.

MAINARDI, F. 2010. *Fractional Calculus and Waves in Linear Viscoelasticity*. Imperial College Press.

MANDELBROT, B. B. 2002. *Gaussian, Self-Affinity and Fractals*. Springer.

NAKAO, M., TAKIZAWA, T., NAKAMURA, K., KATAYAMA, N., AND YAMAMOTO, M. 2001. An optimal control model of 1/f fluctuations in heart rate variability. *IEEE Engi. Medicine Biology Soci. 20,* 2, 77–87.

NEOGI, B., GHOSH, R., TARAFDAR, U., AND DAS, A. 2010. Simulation aspect of an artificial pacemaker. *Int. J. Infor. Technol. Knowl. Manag. 3,* 2, 723–727.

ONARAL, B. AND SCHWAN, H. P. 1982. Linear and nonlinear properties of platinum electrode polarization, part i, frequency dependence at very low frequencies. *Medical Biological Eng. Computa. 20,* 3, 299–306.

OUSTALOUP, A. 1995. *La Derivation Non Entiere: Theorie, Synthese et Applications*. Hermes, Paris.

PhysioNet. The research resource for complex physiologicsignals. http://www.physionet.org/.

PODLUBNY, I. 1999. *An Introduction to Fractional Derivatives, Fractional Differential Equations*. Academic Press.

SANDERS, R. S. AND LEE, M. T. 1996. Implantable pacemakers. *Proc. IEEE 84,* 3, 480–486.

SCHALDACH, M. 1998. What is closed loop stimulation? *Progress Biomed. Res. 3,* 2, 49–55.

SCHULTZ, W. C. AND RIDEOUT, C. V. 1961. Control systems performance measures: Past, present and future stimulation. *IRE Trans. Automatic Control AC- 6*, 22.

SIMANTIRAKIS, E. N., ARKOLAKI, E. G., AND VARDAS, P. E. 2009. Novel pacing algorithms: Do they represent a beneficial proposition for patients, physicians, and the health care system? *Europace 11,* 10, 1272–1280.

SRIDHAR, M. K., SRINATH, R., AND PARTHASARATHY, K. 1987. On the direct parallel solution of systems of linear equations: New algorithm and systolic structures. *Info. Sciences 43,* 1-2, 25–53.

STANGL, K., WIRTZFELD, A., LOCHSCHMIDT, O., BASLER, B., AND MITTNACHT, A. 1989. Physical movement sensitive pacing: Comparison of two activity-triggered pacing systems. *Pacing Clin Elec. 12,* 1, 102–110.

STANKOVIC, J. A., LEE, I., MOK, A., AND RAJKUMAR, R. 2005. Opportunities and obligations for physical computing systems. *Computer 38,* 11, 23–31.

STICHERLING, C., KÜHNE, M., SCHAER, B., ALTMANN, D., AND OSSWALD, S. 2009. Remote monitoring of cardiovascular implantable electronic devices. *Swiss Medical Weekly 139,* 41-42, 596–601.

SUGIURA, T., MIZUSHINA, S., KIMURA, M., FUKUI, Y., AND HARRADA, Y. 1991. A fuzzy approach to the rate control in an artificial cardiac pacemaker regulated by respiratory rate and temperature: A preliminary report. *J. Medical Eng. Technol. 15,* 3, 107–110.

SUGIURA, T., NAKAMURA, Y., AND MIZUSHINA, S. 1983. A temperature-sensitive cardiac pacemaker. *J. Medical Eng. Techno. 7,* 1, 21–23.

SUN, Q., SCHWARTZ, F., MICHEL, J., AND ROM, R. 2008. Implementation study of an analog spiking neural network in an auto-adaptive pacemaker. In *Proceedings of the 6th IEEE Joint NEWCAS (Circuits and Systems)–TAISA (NEWCAS–TAISA'08)*. IEEE, 41–44.

XILINX. Supplier of programmable logic devices. http://www.xilinx.com/.

XilinxDSP. Xilinx - digital signal processing design considerations. http://www.xilinx.com/support/documentation/userguides/ug073.pdf.

ZHANG, Y., MOWREY, K. A., ZHUANG, S., WALLICK, D. W., POPOVIC, Z. B., AND MAZGALEV, T. N. 2002. Optimal ventricular rate slowing during atrial fibrillation by feedback av nodal-selective vagal stimulation. *Amer. J Physiol Heart Circ. Physiol. 282,* 3, 1102–1110.

Received January 2012; revised July 2012; accepted October 2012